Supplementary Material

1. Validation of capillary sag calculations

This section provides information on several tests that were done to validate the computational estimates of sag on glass capillaries due to their own weight. The equations adapted from the theory of flexure for simple beams given in Appendix A have been implemented as a FORTRAN program called SAG. The older calculations in this section do not employ the boundary condition given in Appendix A (6), consequently the computed results were manually rotated and translated to align the endpoints with the experimental conditions.

A tiny hollow quartz glass fiber of 52.3 cm length and of uniform cross section was obtained from Fiberware (Berlin, Germany). The outside diameter was 290 microns and the inside 183 microns in diameter. The fiber was laid onto two round pens supported above a wooden desktop at Hasylab. The displacement vs. length profile was determined with a metal ruler and was probably accurate to 0.3 mm. This is the main experimental error in the data.

The modulus of elasticity was taken for silica glass (fused silica) from E. B. Shand, Glass Engineering Handbook (1958) by Maple Press Company, York, PA and adjusted by 3% in value to better fit the data.

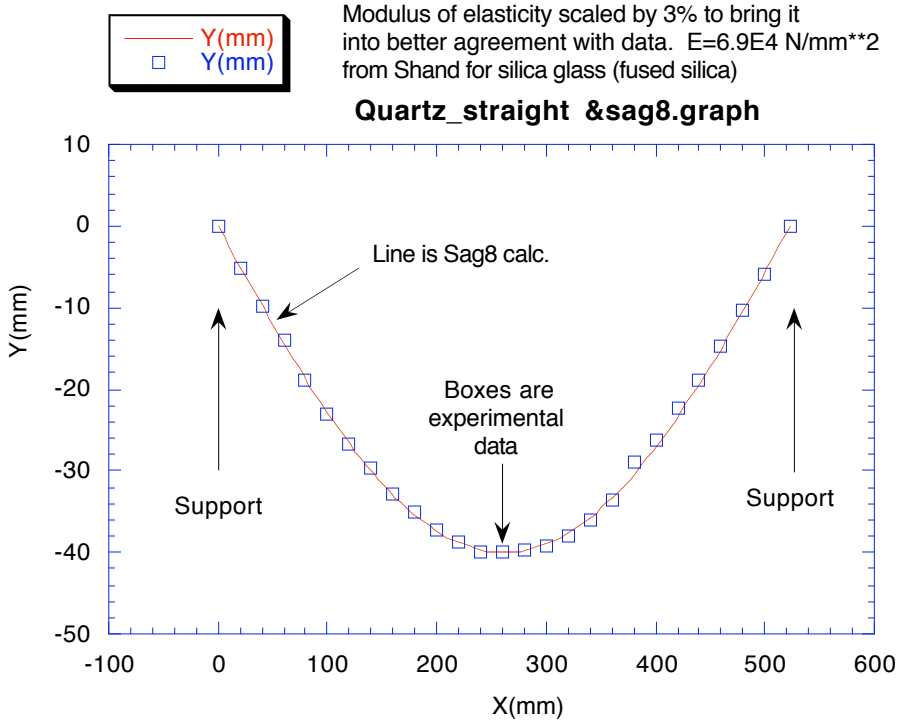

Figure 1. Deflection vs Length for a straight tube of quartz.

The agreement between experiment and theory is excellent (and is in absolute agreement to within 3%).

The second example is taken from a long lead glass fiber pulled from a piece of LG-1 tubing from Detector Technology. Reinhard Pahl pulled the taper on the computerized drawing tower at Cornell University and Donald Bilderback profiled it on an Olympus microscope. The 57 cm long fiber continuously varies in cross section from 966 microns at the base end to 262 microns at the tip. The decrease in diameter from base to tip is approximately a factor of 3.7.

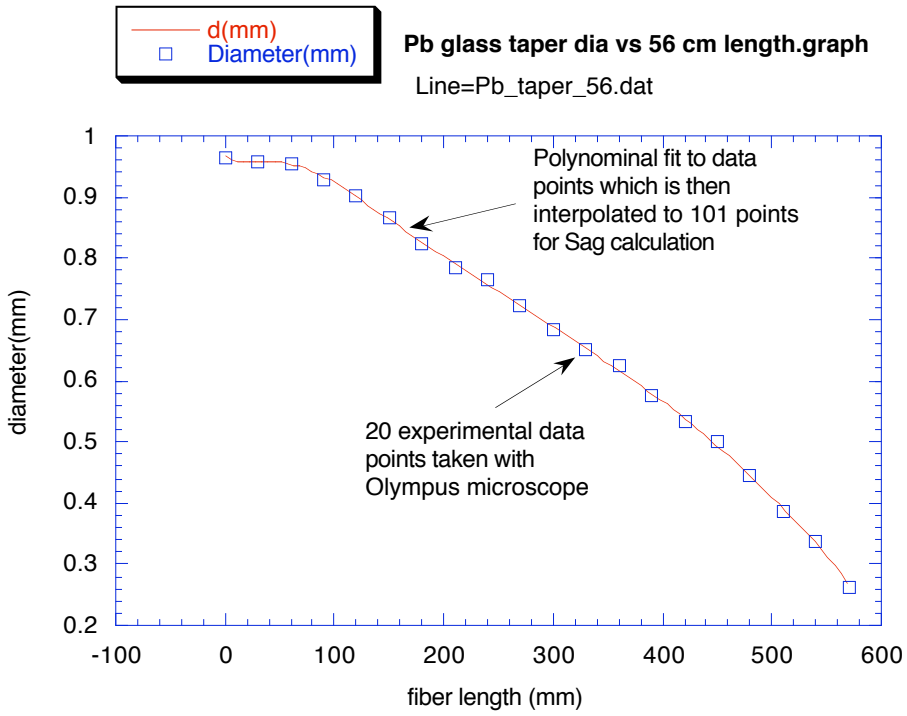

Figure 2. Diameter vs. length profile of tapered leaded glass fiber.

In order to determine the modulus of elasticity, the deflection under gravity of a fiber of uniform cross section was measured. The deflection, y, is given in Machinery Handbook, 22nd edition by E. Obert, Jones, and Horton (1984), Industrial Press Inc., NY as

y = 5/384*WI**3/(E*I) and I = pi/64* (OD**4-ID**4)

where 5/384 is a constant, W is the total weight of capillary assumed to present a uniform load over the length of the capillary, 1 is the length, E the modulus of elasticity, and I, the second moment of area. OD = outside diameter and ID = inside diameter. For a 50.5 cm long tube of 0.97 mm OD observed to sag by 1.27 cm, you calculate E=5.80E4 N/mm**2. Armed with this constant, we can now calculate the sag of the variable cross section of fiber.

This fiber was mounted on supports as before and two more data sets were obtained, one with the supports close together (convex bending) and the other far apart (concave bending).

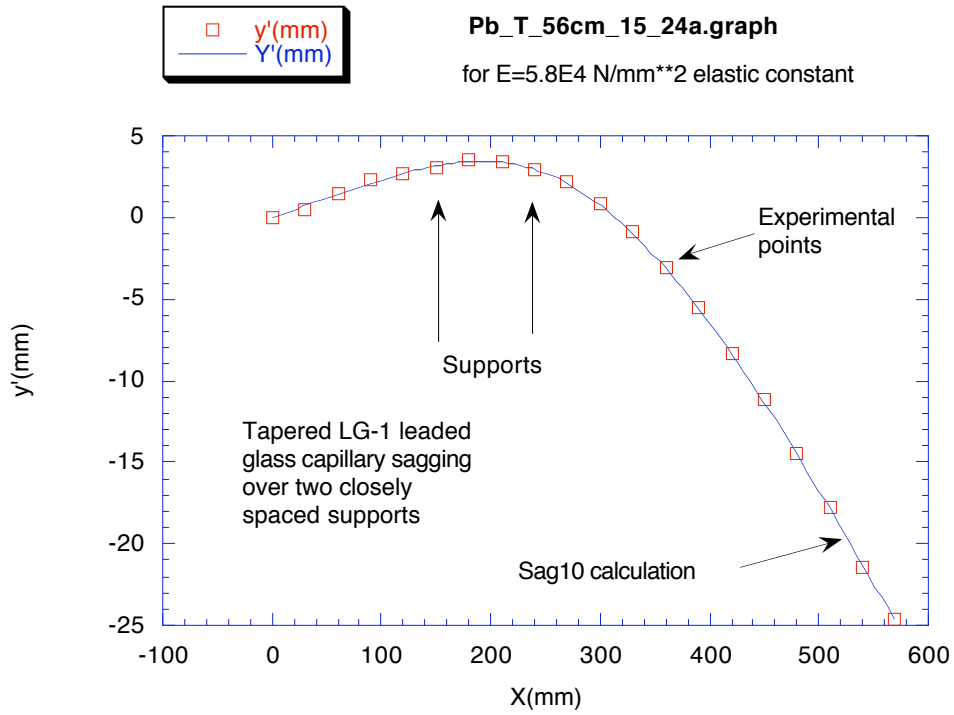

Figure 3. Tapered leaded glass tube whose base is at the left and whose thin tip is at the right. The supports are close together so the flimsy fiber sags downward at both ends under gravity and the curve is convex.

The SAG program gives a calculated shape that can be compared to experiment. This was done by translating and rotating the shape to match the endpoints of the experimental curve. The calculated points and experimental points again agree within the experimental error. Since the modulus of elasticity was determined by earlier experiments, there are no adjustable parameters for this calculation. [The real fiber was slightly bent, but data sets taken with a red mark on the fiber up or down matched to nearly within the experimental error. Thus just one data set is shown].

Next the supports are moved further apart and the last data set was obtained.

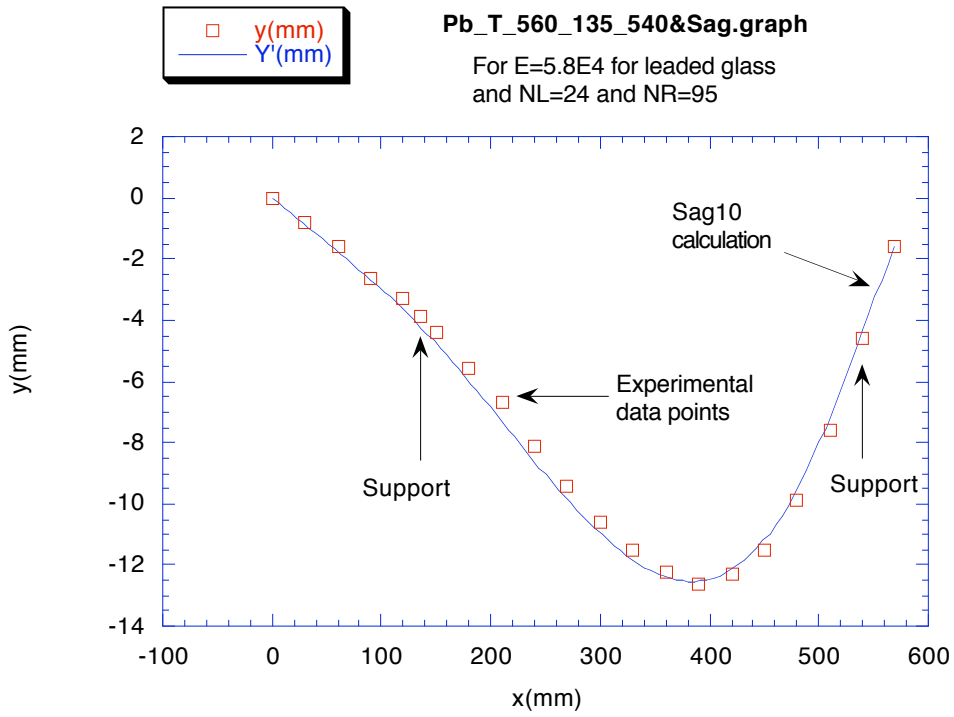

Figure 4. Deflection of tapered glass tube where thick diameter base is supported at x=135 mm and the tip is supported at x=540 mm distance from the base. This time the curve is concave.

The SAG calculated shape was again translated and rotated to match up to the end points of the experimental data. Again, the agreement is excellent between theory and experiment. Please note that the sag in Fig. 4 is about 13 cm as opposed to 28 cm of variation of Fig. 3. This change of scale magnifies the real errors present in the data by about a factor of two between the two data sets.

A version of Sag was made to handle the case of a fiber supported (cantilevered) at one end.

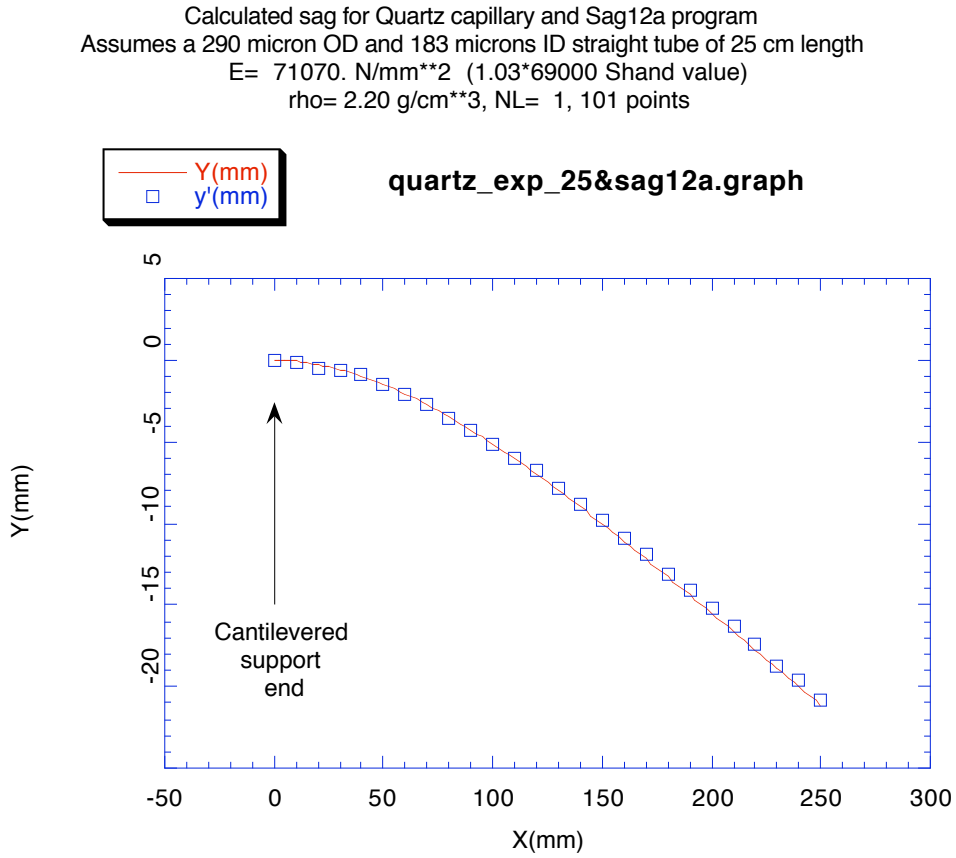

These tests, which show excellent agreement with experimental measurements, provide a basic validation for the method which allows us to confidently apply it to regimes in which the deformations are too small to measure.

2. Background scattering

In the absence background of scattering from sources other than sample, the signal-to-noise ratio can be improved by simply using longer exposures or more intense x-ray beams. Under realistic conditions, however, there are multiple sources of background scatter that also scale with incident intensity; each source of background degrades the signal-to-noise ratio. Background scattering is particularly critical with weaker signals since the observed signal represents the difference between sample and background signals, while the observed noise is the square root of the sum of the sample and background signals (Pflugrath, 1999). Any photons that are not a result of scatter from the protein are a source of unwanted background.

Both slits and aperture-based collimators produce some parasitic background scatter. Since x-rays scatter off of metallic edges, it is common practice in the case of slits to use a set of down-stream guard slits slightly larger than the beam diameter to remove unwanted scatter. Aperture-based collimation suffers from the same phenomenon but

parasitic scatter is often removed by a guard aperture on the collimator-mounted ion chamber. In microcrystallography, apertures near the sample are frequently used in combination with upstream focusing to further define the beam (Fischetti *et al.*, 2009). Capillary optics are based on specular reflection of x-rays from glass at very shallow angles. The glass can be a source of parasitic scatter, including Compton scattering, X-ray fluorescence from trace elements, and small angle scattering from the tip and the base of the optic. A guard aperture can be placed after the optic to eliminate most of the parasitic scattering from the glass (Engstrom & Riekel, 1996). The capillary housing design permits placement of a guard aperture 10 mm from the end of the capillary, leaving 12 mm of working distance to the sample. The short distance between the sample and the guard aperture minimizes air scatter, and places the aperture just outside the coldstream.

A guard aperture of 500 μm restricts the parasitic scatter to below 25Å resolution on CCD images, a value which is adequate for most macromolecular crystallography. To estimate the degree to which parasitic scattering is important, we can compare CCD images taken before and after placement of the guard aperture.

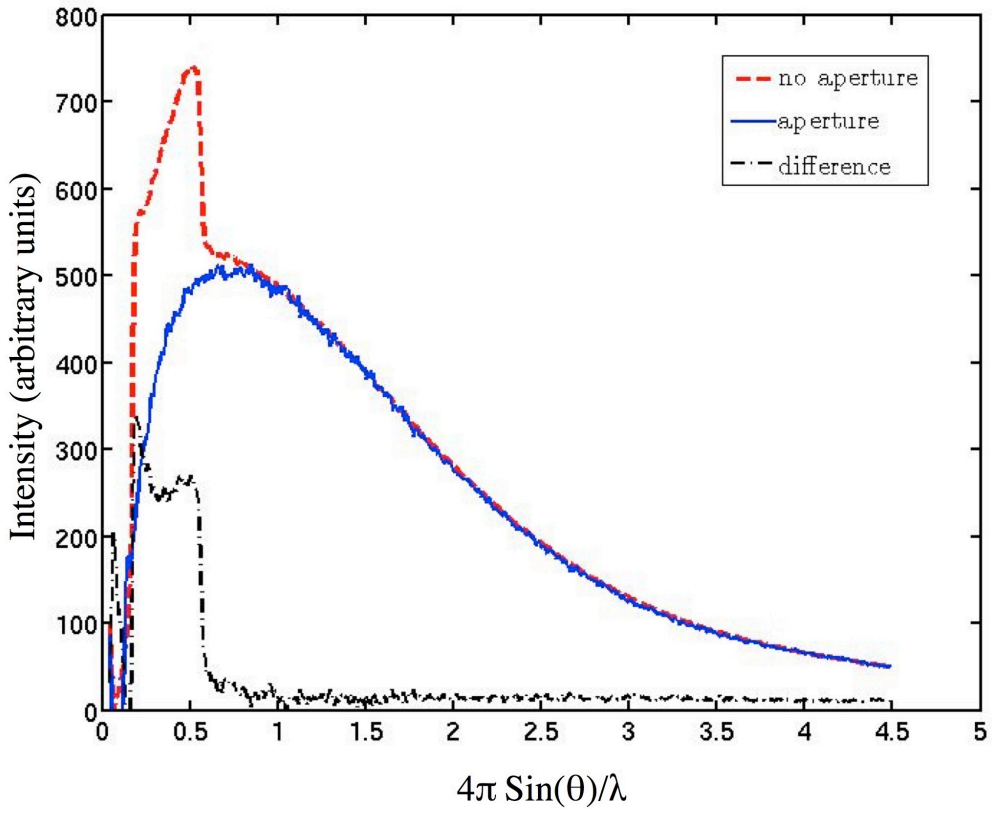

The figure above is a superposition of the radial profiles with and without aperture. Note that the construction of the capillary housing by itself already blocks scatter up to 10.5 Å ($4\pi\mathrm{Sin}(\theta)/\lambda > 0.6$), consequently only the low-angle portion of the parasitic scatter is

visible in this experiment. The difference shows that unblocked parasitic scatter accounts for 1/3 to 1/2 of the signal in these low-angle regions.

A final potential source of scatter for some capillary configurations comes indirectly as a result of unfocused direct beam. By nature, capillaries are hollow and x-rays, if unblocked, are free to pass through the centre of the optic. In general, these unfocused x-rays have a low intensity compared to focused radiation, however, the amount of material they illuminate depends upon the internal diameter of the capillary tip and the way in which the sample is mounted. Large diameter capillaries will illuminate larger sample regions with unfocused beam and thus potentially contribute more to unwanted background scatter. In such cases, it may be necessary to block direct beam using a small beam-block, upstream slits, or apertures.

References

Engstrom, P. & Riekel, C. (1996). Rev. Sci. Instrum. **67**, 4061-4063.

Fischetti, R. F., Xu, S., Yoder, D. W., Becker, M., Nagarajan, V., Sanishvili, R., Hilgart, M. C., Stepanov, S., Makarov, O. & Smith, J. L. (2009). J. Synchrotron Rad. **16**, 217-225.

Pflugrath, J. W. (1999). Acta Cryst. D **55**, 1718-1725.